

Genome architecture and selective signals compensatorily shape plastic response to a new environment

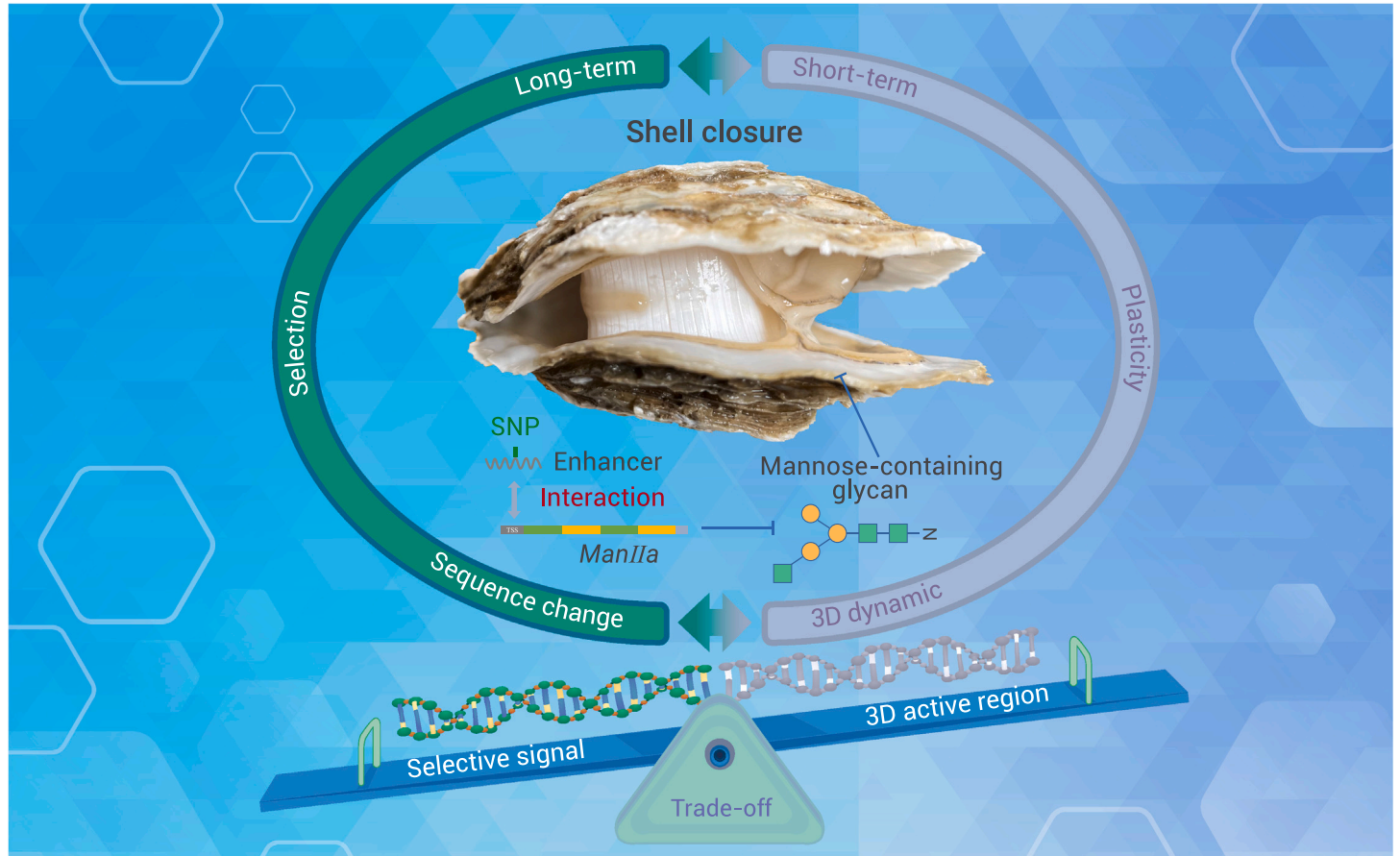
Ao Li,^{1,2,3} Mingjie Zhao,^{1,4} Ziyang Zhang,^{1,4} Chaogang Wang,^{1,4} Kexin Zhang,^{1,4} Xu Zhang,⁵ Pierre Raoul De Wit,⁶ Wei Wang,^{1,2,3,7,8} Juntao Gao,⁵ Ximing Guo,⁹ Guofan Zhang,^{1,2,3,7,8,*} and Li Li^{1,2,3,4,7,8,*}

*Correspondence: gfzhang@qdio.ac.cn (G.Z.); lili@qdio.ac.cn (L.L.)

Received: December 29, 2022; Accepted: June 19, 2023; Published Online: June 21, 2023; <https://doi.org/10.1016/j.xinn.2023.100464>

© 2023 The Authors. This is an open access article under the CC BY-NC-ND license (<http://creativecommons.org/licenses/by-nc-nd/4.0/>).

GRAPHICAL ABSTRACT



PUBLIC SUMMARY

- 3D genome structure affects oyster's transcriptional plasticity upon environmental change.
- 3D architecture compensates for sequence variations during environmental responses.
- Mutation, lincRNA, and accessibility of an enhancer regulate *ManIIa* expression.
- *ManIIa* controls muscle function, shell closure, and environmental adaptation of oysters.



Genome architecture and selective signals compensatorily shape plastic response to a new environment

Ao Li,^{1,2,3} Mingjie Zhao,^{1,4} Ziyang Zhang,^{1,4} Chaogang Wang,^{1,4} Kexin Zhang,^{1,4} Xu Zhang,⁵ Pierre Raoul De Wit,⁶ Wei Wang,^{1,2,3,7,8} Juntao Gao,⁵ Ximing Guo,⁹ Guofan Zhang,^{1,2,3,7,8,*} and Li Li^{1,2,3,4,7,8,*}

¹CAS and Shandong Province Key Laboratory of Experimental Marine Biology, Center for Ocean Mega-Science, Institute of Oceanology, Chinese Academy of Sciences, Qingdao 266071, China

²Laboratory for Marine Biology and Biotechnology, Laoshan Laboratory, Qingdao 266237, China

³Key Laboratory of Breeding Biotechnology and Sustainable Aquaculture, Chinese Academy of Sciences, Wuhan 430072, China

⁴University of Chinese Academy of Sciences, Beijing 100049, China

⁵Department of Automation, Tsinghua University, Beijing 100084, China

⁶Department of Marine Sciences, University of Gothenburg, Stromstad 45296, Sweden

⁷National and Local Joint Engineering Key Laboratory of Ecological Mariculture, Institute of Oceanology, Chinese Academy of Sciences, Qingdao 266071, China

⁸Shandong Technology Innovation Center of Oyster Seed Industry, Qingdao 266000, China

⁹Haskin Shellfish Research Laboratory, Department of Marine and Coastal Sciences, Rutgers University, Port Norris, NJ 08349, USA

*Correspondence: gfzhang@qdio.ac.cn (G.Z.); lili@qdio.ac.cn (L.L.)

Received: December 29, 2022; Accepted: June 19, 2023; Published Online: June 21, 2023; <https://doi.org/10.1016/j.xinn.2023.100464>

© 2023 The Authors. This is an open access article under the CC BY-NC-ND license (<http://creativecommons.org/licenses/by-nc-nd/4.0/>).

Citation: Li A., Zhao M., Zhang Z., et al., (2023). Genome architecture and selective signals compensatorily shape plastic response to a new environment. *The Innovation* 4(4), 100464.

Transcriptional plasticity interacts with natural selection in complex ways and is crucial for the survival of species under rapid climate change. How 3D genome architecture affects transcriptional plasticity and its interaction with genetic adaptation are unclear. We transplanted estuarine oysters to a new environment and found that genes located in active chromatin regions exhibited greater transcriptional plasticity, and changes in these regions were negatively correlated with selective signals. This indicates a trade-off between 3D active regions and selective signals in shaping plastic responses to a new environment. Specifically, a mutation, lincRNA, and changes in the accessibility of a distal enhancer potentially affect its interaction with the *Man1a* gene, which regulates the muscle function and survival of oysters. Our findings reveal that 3D genome architecture compensates for the role of genetic adaptation in environmental response to new environments and provide insights into synergetic genetic and epigenetic interactions critical for fitness-related trait and survival in a model marine species.

INTRODUCTION

Rapid climate change poses a serious threat to global biodiversity and ecosystem functions. Therefore, the survival of organisms increasingly depends on their ability to respond to novel environmental conditions in real time. Phenotypic plasticity, which is a single genotype that produces various phenotypes in different environments, is a widespread adaptive strategy for short-term environmental fluctuations.^{1,2} Transcriptional plasticity is commonly used to explore the relationship between plastic change and evolutionary adaptation,^{3–5} another form of organismal responses to environmental disturbance via allele frequency changes. However, to what extent and under what conditions transcriptional plasticity facilitates or impedes evolutionary adaptation remains controversial. Plastic changes can serve as emergency responses, irrespective of the fitness, and are often necessary for organism survival; they reduce the risk of extinction and provide time for organisms to achieve optimal fitness.^{2,6,7} This adaptive plasticity exists only when the modified environment is similar to the organism's native or ancestral environments.^{3,8} Selection favors adaptive plastic changes that are highly sensitive to reliable environmental cues.^{9–13} Ongoing stabilizing or purifying selection eliminates standing genetic variations for traits with a high degree of adaptive transcriptional plasticity under stable long-term environmental conditions.^{12,13} However, some studies have found that plastic responses compensate for rather than strengthening genetic adaptation, resulting in maladaptive plasticity due to the mismatch between gene expression and an environment that the organisms have not experienced previously.^{4,5,14} These mismatched plastic changes to novel environments can evolve via genetic accommodation.^{15,16} However, the mechanistic basis for the interplay between maladaptive plastic responses and selection is unclear.

Theoretical and empirical work has documented that there exists a regulatory interaction between genomic variation and plasticity. Genome-wide studies have revealed that many environmentally responsive or fitness-related loci are located

within noncoding or intergenic genomic regions rather than within coding sequences.^{9,10,17,18} In particular, distal upstream regulatory elements, such as enhancers, rather than local promoters, have been found to be under selection and show adaptive divergence among populations distributed across spatiotemporal environmental gradients.^{7,18} The interaction between genomic variation and plasticity is specified by sequence diversity in these distal regulatory elements, which can modulate the expression of downstream genes and underlie transcriptional plasticity.^{7,12,17} Knowledge of the genome topology and local chromatin accessibility can illustrate how variations in regulatory elements affect gene expression plasticity.

The three-dimensional (3D) configuration of the genome is complex and important for DNA transcription, replication, recombination, and repair, and affects many biological processes. In addition to its basic nucleosome-level organization, the chromatin is further organized into chromatin loops, topologically associated domains (TADs), relaxed or compact compartments, and chromosome territories, which comprise prevalent epigenetic features that can affect nuclear function, gene expression, and many cellular functions.^{19–24} Although 3D chromatin topology and accessibility regulate gene expression during development and disease,^{25–27} how variations in genome architecture contribute to transcriptional plasticity under environmental change is poorly understood. It is also unknown whether environmental changes alter the 3D genome architecture and re-orchestrate plasticity as a general mechanism of the environmental response. Recent advances in sequencing technologies, such as whole genome next-generation sequencing, Hi-C sequencing, and assay for transposase-accessible chromatin sequencing (ATAC-seq), have facilitated high-resolution studies of the signatures of selection and 3D genome interactions in non-model species. Elucidating environmentally induced changes in chromatin topology and accessibility can deepen our understanding of the plastic capacity of marine organisms under climate change.

Recent studies have shown that standing genetic variation increasing plastic responses can help organisms, especially estuarine invertebrates, to adapt to unfamiliar environments, and genome organization plays a critical role in shaping this interaction between genomic variation and plasticity.^{28,29} Oysters are ecologically and economically important bivalve molluscs that inhabit estuarine and intertidal zones, and they experience sharp environmental fluctuations, especially in temperature and salinity, owing to the tide cycle.^{30,31} As sessile organisms incapable of active movement, oysters^{10,11,32} and other intertidal or shallow sea species^{33–35} have evolved high genetic diversity and plasticity to cope with rapid changes in ambient conditions. Closely related species and different populations within the same species have evolved divergent genomic structure and plastic responses, which contributes to adaptation to environmental gradients.^{9–11} In particular, the estuarine oyster *Crassostrea ariakensis* is broadly distributed in China, spanning over 20° latitudes and exposed to substantial fluctuations in temperature and salinity from northern to southern habitats.^{9,36} Based on reciprocal transplant experiments, it was found that oysters derived from northern habitats can barely survive in southern environments with elevated temperatures, even for a short-term culture during summer.³⁶ This indicates that

environmentally induced plastic responses cannot bring oysters closer to optimal fitness. Genome-wide sequencing studies have revealed that the northern and southern populations have evolved strong genetic variations. Moreover, directional selection prefers to act on environmentally responsive genes, and noncoding regions exhibit higher genomic divergence than coding regions, especially in upstream intergenic regions.^{9,10} These findings highlight the association between plasticity and regulatory elements and their significance in the environmental adaptation of oysters.

In bivalves, shell closure is the first physical barrier in response to changes of ambient conditions. As an important fitness trait, the bivalves swiftly close their shells when they encounter environmental stresses, which can also be an indicator of health status in bivalves.^{37,38} Oysters that maintain tight shell closure, such as *Crassostrea virginica*, survive better under hypoxia and air exposure than other oysters, such as *C. ariakensis*, that do not.^{39,40} Two types of adductor muscles, smooth and striated, play important roles in this response.⁴¹ Smooth muscle generates the force to keep shells closed tightly for long periods, whereas striated muscle facilitates the rapid and repetitive opening and closing of shells.^{38,42} The paramyosin-rich thick filaments in smooth muscle contribute to its catch tension, and the fusion dynamics of filaments affects catch contractions.^{42,43} However, the molecular regulation of shell closure is not well understood, and whether this trait yields environmental plasticity that involves changes in chromatin topology and accessibility changes is unknown.

In this study, the estuarine oyster was used to investigate how 3D chromatin configuration affects transcriptional plasticity and fitness, as determined by the function of muscles. An analysis of 3D genome patterns in oysters translocated from a native northern habitat to a non-native southern environment provided the dynamics of the chromatin topology landscape during environmental change. In addition to providing a link between 3D genome architecture and selective signals, our findings revealed that chromatin 3D topology is an important regulatory mechanism of transcriptional plasticity, which interacts with selective signals to regulate fitness-related traits in estuarine oysters in a cooperative manner. This may be a general mechanism important for the environmental adaptation of marine organisms to rapid climate change.

RESULTS

Characterization of the high-order structure of the oyster genome

To investigate the role of 3D chromatin structures in the response of marine molluscs to environmental changes, we conducted *in situ* Hi-C and RNA sequencing in estuarine oysters from northern China (Bohai Sea) and those translocated to southern China (South China Sea).⁴⁴ Biological replicates from the same environments showed higher association scores between each other than those from different environments (Table S1).

We constructed a Hi-C map to examine genome packing at the chromosomal level at a low resolution (200 kb). The map showed strong contact signals along the diagonal, representing intra-chromosomal contacts (Figures 1A and S1). Intra-chromosomal (*cis*-) contacts were approximately 2.00- to 3.18-fold higher than inter-chromosomal (*trans*-) contacts (Table S2), although the frequency of *cis*-interactions decreased rapidly with linear distance (Figure S2).

After inspecting the high-order structures of the oyster genome through a principal-component analysis, chromatin regions in each chromosome were organized into A and B compartments corresponding to active and inactive regions,⁴⁵ respectively (Figure 1A). There was a higher ratio of genomic regions in compartment A than in compartment B (Table S3). We generated a contact map using 20 kb bins to examine the local patterns of chromatin packing at higher resolution. A visual inspection revealed that oyster genomes were further organized into TADs (Figure 1A). We identified 2,923 and 2,893 TADs in oysters living in the northern and southern environments, respectively (Table S3). Furthermore, A compartments and TAD boundaries displayed higher gene densities than B compartments and intra-TAD regions in both environments (Figure 1B). Genes within A compartments exhibited significantly higher expression levels than those in B compartments ($p < 0.001$, Wilcoxon rank-sum test, Figure 1C). Gene expression was significantly higher in oysters from the non-native southern environment than in those from the native northern environment in all compartments (Figure 1C). There were no differences in the expression of genes located in the intra-TAD regions and of those at TAD boundaries ($p > 0.05$; Figure 1C).

To explore transcriptional regulation mediated by chromatin accessibility, we performed ATAC-seq to identify open chromatin regions across the genome.

ATAC-seq peaks were enriched near the TAD boundaries (Figure S3) and highly enriched around the transcriptional start site for all oyster samples (Figure S4A). Over 60% of the peaks were in putative promoter and intergenic noncoding regions (Figure S4B). Genes adjoining accessible regions showed significantly higher expression than those in compact chromatin regions ($p < 0.001$; Figure S5). The oysters from the non-native southern environments also exhibited significantly higher gene expression than those from the native northern habitats ($p < 0.001$; Figure S5).

Chromatin topology differences associated with environmental conditions

We found that 9.4% (26.6 Mb) of the A compartments switched to B and 10.7% (31.4 Mb) of the B compartments switched to A when oysters were translocated from the native northern habitat to the non-native southern environment. Furthermore, 0.8% (4.8 Mb) of the intra-TAD regions switched to TAD boundaries, whereas 84.6% (5.6 Mb) of the TAD boundaries switched to intra-TAD regions (Table S4). There were dynamic changes in the types and matching frequencies of the sequence motifs at the TAD boundaries, which were also associated with the ATAC-seq peaks, when the oysters were translocated to the non-native environment (Table S5). Several motifs that were recognized as transcription factors, including UNC-86 and UNC-62 that show RNA polymerase II *cis*-regulatory region sequence-specific DNA-binding activity, were enriched in the oysters translocated to the non-native environment ($p \leq 1.40E^{-13}$).

We investigated the dynamics of genome-wide gene expression profiles during environmental translocation and observed divergent expression patterns between oysters dwelling in the native and translocated environments (PC1 = 52.1%; Figure 1D). A total of 1,095 and 711 differentially expressed genes (DEGs) (6.09% of the genome) were significantly upregulated and downregulated, respectively ($p < 0.05$, fold change > 1.5), following the environmental change. A total of 398 DEGs were associated with 3D structure alterations in the genome. A large fraction (62.2%, 1,023 out of 1,806) of the DEGs were adjacent with accessible regions (Figure S6).

Among the DEGs associated with 3D structure alterations (compartments or TAD switch) or adjacent to accessible regions, those involved in energy metabolism were significantly enriched ($p < 0.05$, Table S6). The genes involved in lipolysis (fatty acid degradation) were highly expressed in the non-native southern environment, whereas those involved in carbohydrate metabolism (glycolysis, pyruvate metabolism, and the citrate cycle) were highly expressed in the native northern habitat (Figure S7).

A higher ratio of DEGs was observed in the stable A compartment, TAD boundaries, and regions that changed into A compartments and TAD boundaries after translocation than in the other regions (Figure 1E). Of the four types of chromatin topology changes, genes in genomic regions that recruited topological switches of B-to-A compartments and intra-to-boundary TADs exhibited higher plasticity when oysters were translocated to the non-native environment (Figure 1F).

Relationship between selective signals and chromatin topology alterations

To explore the relationship between genetic adaptation due to long-term divergent evolution and changes in chromatin topology after short-term environmental changes, we scanned whole-genome variations to identify genomic regions under selection between wild native populations of the northern and southern environments.⁹ The “3D response regions” were defined as changes in active genomic regions, including those in the A compartments and TAD boundaries, when oysters were translocated to the non-native southern environment. The lengths and number of genes within the 3D response regions and under selection were measured at the chromosomal level, along with the average F_{ST} value and plasticity of gene expression, to assess the relationship between adaptive evolution and environmental response.

Genomic regions exhibiting selective sweep signals ranged from 0.10 to 3.23 Mb among the 10 chromosomes. The sizes of the regions under selection and 3D response regions were not correlated with chromosomal length ($p > 0.05$, $\rho_{\text{selection}} = 0.32$, $\rho_{\text{compartment A}} = -0.55$, $\rho_{\text{TAD boundary}} = -0.09$, Spearman correlation; Figure 2A). Chromosomes with large regions under selection showed decreased 3D response regions after environmental translocation (Table S7). There was a significantly negative association between genomic length under selection and in the 3D response regions of the A compartments ($p = 0.0018$,

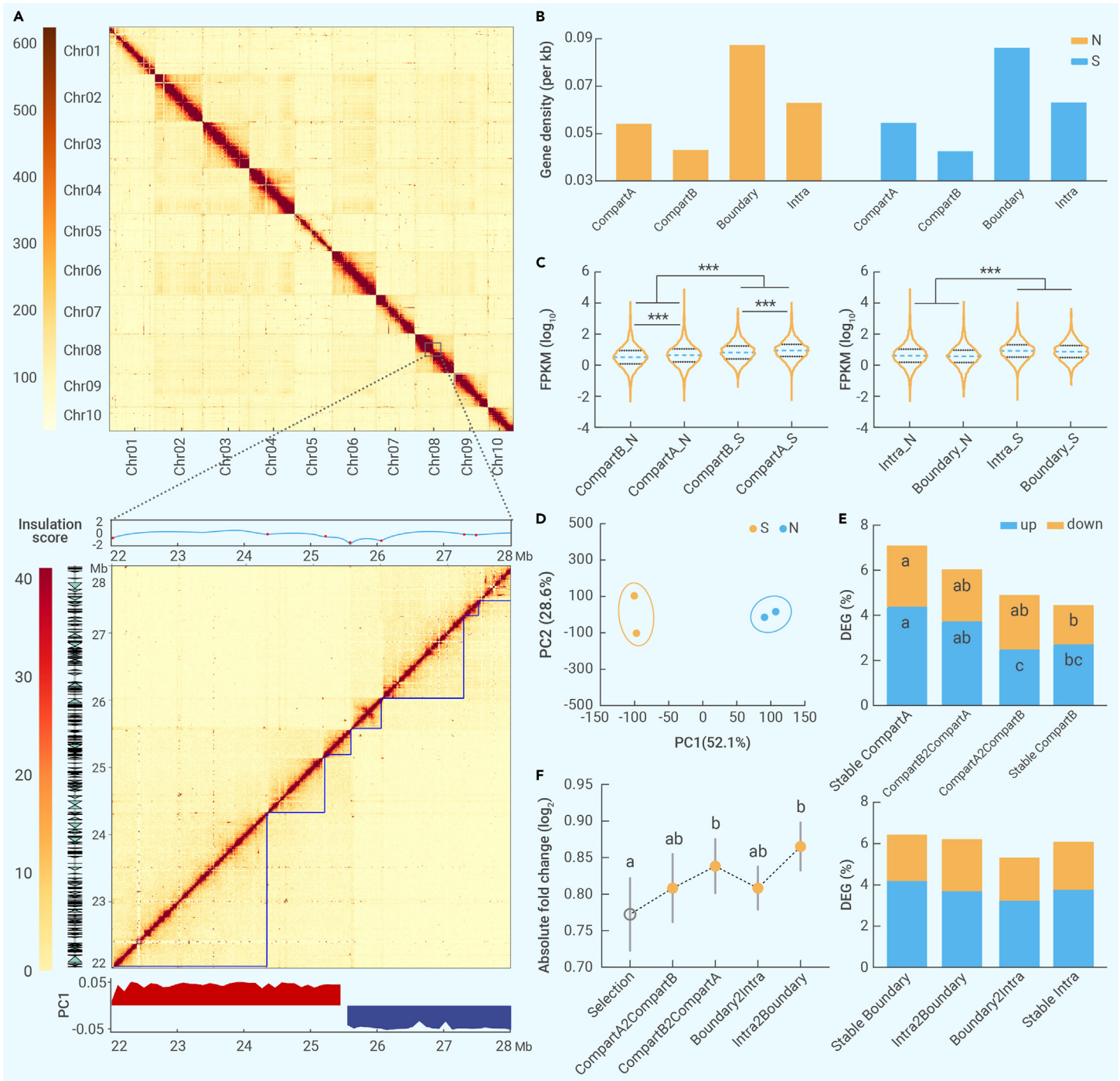


Figure 1. Characteristics of the 3D architecture of the oyster genome under environmental changes (A) Hi-C contact heatmap for 10 oyster chromosomes in the native (northern) habitat at 200 kb resolution (top), with a zoomed-in 6-Mb region of chromosome 8 at 20 kb resolution (bottom). Gene models are indicated by blue triangles on the left of the heatmap. Compartments A (red) and B (blue) were classified using the first principal component from HOMER at the bottom of the heatmap. TADs are identified by insulation scores at the top of the heatmap and marked by blue lines inside. (B) Gene density for genomic regions belonging to compartments A (compartmentA) and B (compartmentB) and TAD boundaries (Boundary) and intra-TAD (Intra) in oysters from the northern (N) and southern (S) environments. (C) Expression levels (\log_{10} (FPKM)) of genes in compartments A (compartmentA) and B (compartmentB) and TAD boundaries (Boundary) and intra-TAD (Intra) of oysters from the northern (N) and southern (S) environments. Data are presented as violin plots. The black and bold blue dashed lines denote the first quartile, median, and third quartile of the data. (D) Principal-component analysis (PCA) plot for genome-wide gene expression profiles of oysters sampled from the northern (N) and southern (S) environments. (E) Percentage of differentially expressed genes (DEGs) in genomic regions where compartments and TADs were changed (compartmentA2compartmentB, compartmentA to compartmentB; compartmentB2compartmentA, compartmentB to compartmentA; Intra2Boundary, TAD-intra to TAD boundary; Boundary2Intra, TAD boundary to TAD-intra) and unchanged (stable compartmentA/compartmentB and stable Intra/Boundary) when the oysters were translocated from the northern to southern environments. (F) Plasticity of genes (\log_2 [absolute fold change]) in genomic regions and under selection or where compartments and TADs were changed upon oyster translocation. (C and E) The left/up and right/bottom panels represent compartments and TADs, respectively. Asterisks and different letters indicate significant differences ($***p < 0.001$). The error bars represent standard error of the mean (SEM) values.

$\rho = -0.85$) and TAD boundaries ($p = 0.0077$, $\rho = -0.78$) (Figure 2A). Furthermore, the number of genes in the regions under selection and 3D response regions in the A compartments ($p = 0.0038$, $\rho = -0.82$) and TAD boundaries ($p = 0.0032$, $\rho = -0.83$) were negatively correlated at the chromosomal level, whereas the total gene number per chromosome was positively correlated

with the number of genes under selection ($p = 0.0061$, $\rho = 0.79$) but was negatively correlated with that in the 3D response regions in TAD boundaries ($p = 0.030$, $\rho = -0.68$) (Figure 2B).

We examined the relationship between F_{ST} and plasticity at the chromosomal level and detected robust negative associations ($p = 0.038$, $\rho = -0.66$; Figure 2C).

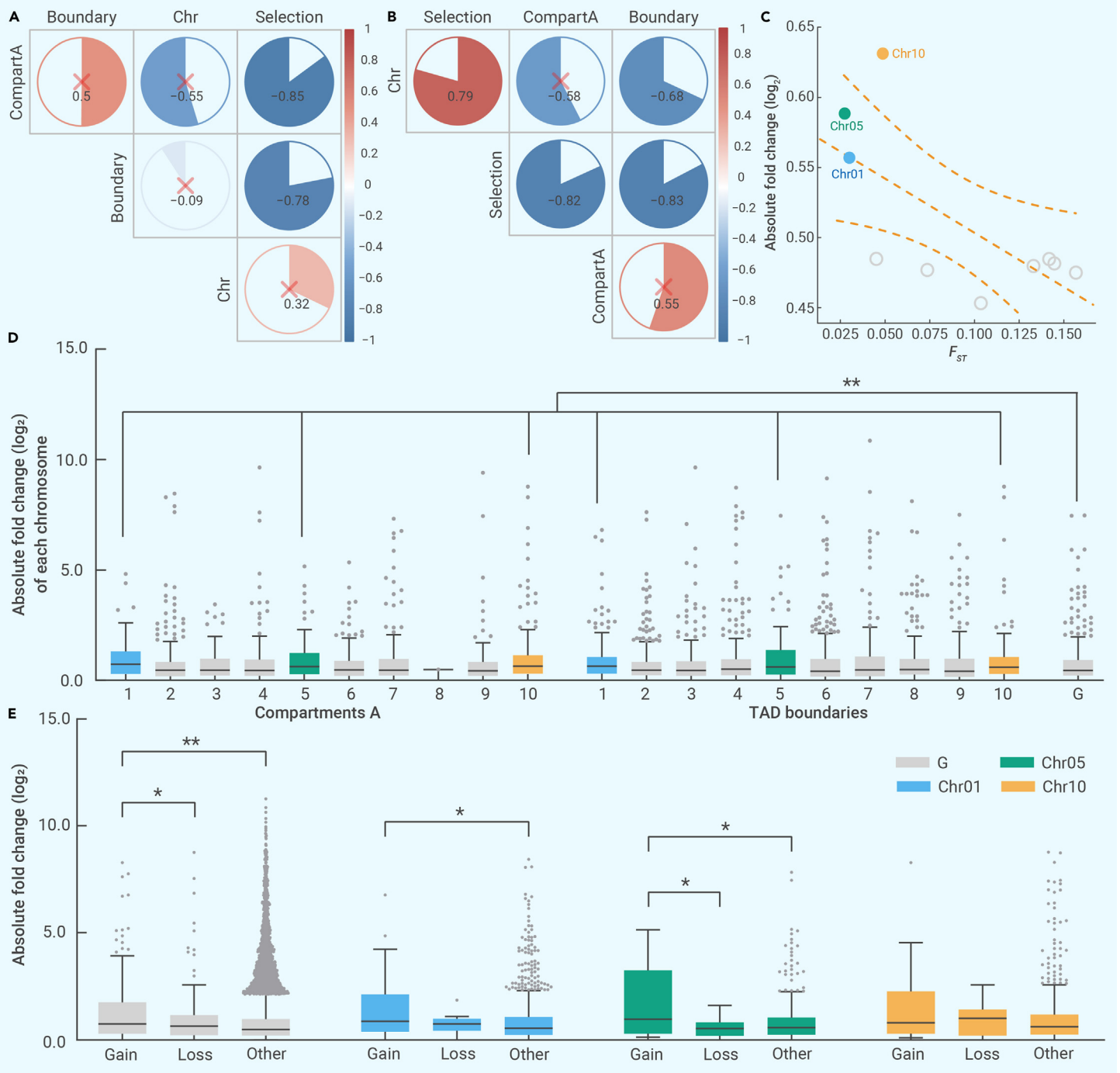


Figure 2. Relationships between long-term genomic evolution and short-term chromatin topological alterations and characterization of chromosomal plasticity (A and B) Correlations among (A) the length and (B) gene number of each chromosome (Chr) and genomic regions under selection (Selection) and with changes in compartments A (CompartmentA) and TAD boundaries (Boundary) when oysters were translocated to non-native environments. The red \times indicates that correlation is not significant. (C) Relationship between gene expression plasticity and fixation index (F_{ST}) of each chromosome. The straight and curved dashed lines show the fit and 95% confidence intervals, respectively. (D) Plasticity (\log_2 [absolute fold change]) of genes in genomic regions with changes in compartments A (left 10 bars) and TAD boundaries (middle 10 bars) for each chromosome and selective signals in the genome (G). (E) Plasticity (\log_2 [absolute fold change]) of genes adjoining altered (gain or loss) and invariably (other) accessible regions in the whole genome (G, gray) and chromosomes 1 (blue), 5 (green), and 10 (orange). Data are presented as boxplots; the central rectangle spans the first to third quartiles of the distribution, and the "whiskers" above and below the box show the maximum and minimum estimates. The line inside the rectangle denotes the median, whereas dots represent outliers. The asterisks indicate significant differences (* $p < 0.05$, ** $p < 0.01$, *** $p < 0.001$).

Chromosomes 1, 5, and 10 had a higher plastic capacity, ranging from 0.56 to 0.63 (median), than the other chromosomes; however, they exhibited a lower selective sweep signal with F_{ST} values ranging from 0.027 to 0.048 (median) (Figure 2C). Furthermore, we investigated the contribution of genes in the 3D response regions to the plasticity of each chromosome. The genes in the 3D response regions of the A compartments of these three chromosomes exhibited higher plasticity, ranging from 0.64 to 1.0 (median). Those with altered TAD boundaries on chromosomes 5 and 10 exhibited higher plasticity, ranging

from 0.64 to 0.72 (median). Plasticity induced by these topological changes was significantly higher than that of the genes under selection ($p < 0.01$; Figure 2D).

To explore whether the changes in the open chromatin peaks were connected to increased plasticity when the oysters were translocated to the non-native environment, we compared the plasticity of the genes closest to differentially (gain or loss) and invariably (other) accessible regions at the whole-genome and chromosomal levels. The gene-adjoining regions that gained accessibility exhibited

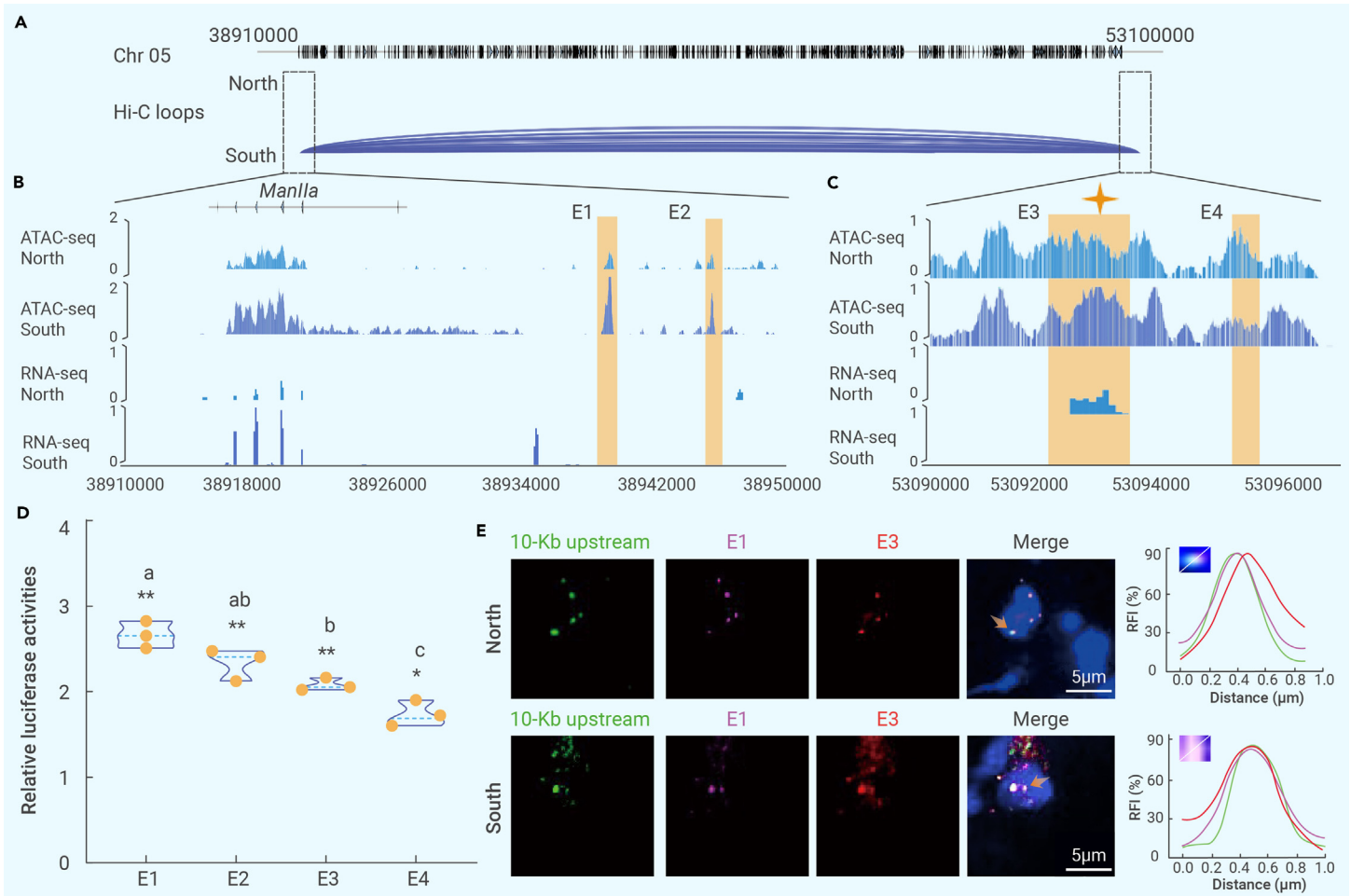


Figure 3. Chromatin interactions, accessibility, and transcription associated with *ManIIa* (A) Hi-C contact map between the 20 kb upstream region and 14.17 Mb noncoding region of *ManIIa*. Gene models are shown as blue triangles. (B and C) ATAC-seq and RNA-seq tracks of *ManIIa* and its 20 kb upstream noncoding region (B) and the predicted interacted genomic regions at 14.17 Mb upstream (C) for oysters from native northern and non-native southern environments. Calling of ATAC-seq and RNA-seq accounts for both replicates. (D) Validation of four enhancers associated with *ManIIa* using a Dual-Luciferase Reporter Assay System in human 293T cells (n = 3). Different letters and asterisks indicate significant differences (*p < 0.05, **p < 0.01; two-tailed Student's t test without multiple comparisons for each enhancer and ANOVA for multiple comparisons among four enhancers). (E) Tn5-FISH of predicted chromatin interactions between the predicted enhancers (E1 and E3) and 10 kb upstream region of *ManIIa*. RFI is the relative fluorescent intensity of dots indicated by orange arrows in the merged images.

significantly higher plasticity than the adjoining regions that were losing accessibility or unaltered at the genome level. Similar results were observed for chromosomes 1 and 5 ($p < 0.05$, Wilcoxon rank-sum test; Figures 2E and S8).

Changes in chromatin interactions and the accessibility of the *ManIIa* gene

We evaluated chromosomes 1 and 5, which evolved higher plasticity not only at the chromosome level and in the active genomic regions of A compartments and TAD boundaries, but also in regions that gained access to chromatin. A total of 14 gene-adjointing regions that gained accessibility showed changes in chromatin topology (Figure S9A). Only one gene, annotated as *class II alpha-mannosidase (ManIIa)*, showed differential expression, changes in chromatin topology, including switches from B-to-A compartment, loop shifts, and changes in the accessibility of adjoining genomic regions in response to environmental change (Figures 3A and 3B). The transcription of *ManIIa* was significantly upregulated ($\log_2[\text{fold change}] = 1.73$, $p = 0.019$) when oysters were translocated to the non-native southern environment (Figure S9B).

We scanned the genomic regions with changes in chromatin interactions between 20 kb upstream noncoding regions of *ManIIa* and other noncoding regions within chromosome 5, as well as those with changes in chromatin accessibility, to identify candidate enhancers that could interact with transcription factors and regulate gene expression. Two differentially accessible regions (DARs) in the 12.86 kb (E1) and 19.51 kb (E2) upstream regions were identified as potentially proximal enhancers ($p < 0.05$; Figure 3B). We identified noncoding loop formations in the 5 kb upstream regions of this gene and two DARs in loop in the

14.167-Mb (E3) to 14.168-Mb (E4) upstream region ($p < 0.05$; Figure 3C), thus predicting two distal enhancers.

Furthermore, we conducted a dual-luciferase reporter assay and found significantly increased transcriptional activities for all four predicted enhancers ($p < 0.05$, Student's t test), whereas the two proximal enhancers (E1 and E2) showed significantly higher activities than the two distal enhancers (E3 and E4) ($p < 0.001$; Figure 3D). Tn5-FISH confirmed the interactions between the predicted enhancers (proximal E1 and distal E3) and 10 kb upstream noncoding regions of *ManIIa*. The proximal E1 interacted with the upstream region of *ManIIa* in both the native and non-native environments. However, the distal E3 showed weak or no interactions with the upstream region of *ManIIa* in the native environment. New and strong interactions were formed after translocation to the non-native southern environment (Figure 3E). We further found that the E3 sequence could be transcribed to a long intergenic noncoding RNA (lincRNA_E3) in the native habitat but not in the non-native environment (Figure 3C).

Expression regulation of *ManIIa* by a selective locus in E3

To investigate the role of E3 in regulating *ManIIa* expression, we assessed this genomic region to predict regulatory element motifs that could bind to transcriptional factors and identified genomic variants (single-nucleotide polymorphisms [SNPs]) in these motifs that exhibited divergent allele frequencies between native northern and southern populations.⁹ We identified one motif in E3 that was predicted to bind to the transcription factor UNC-62 (Figure 4A). An SNP (C/A) in this motif that shows significantly divergent allele frequencies between the native northern and southern oysters was detected. All southern oysters contained

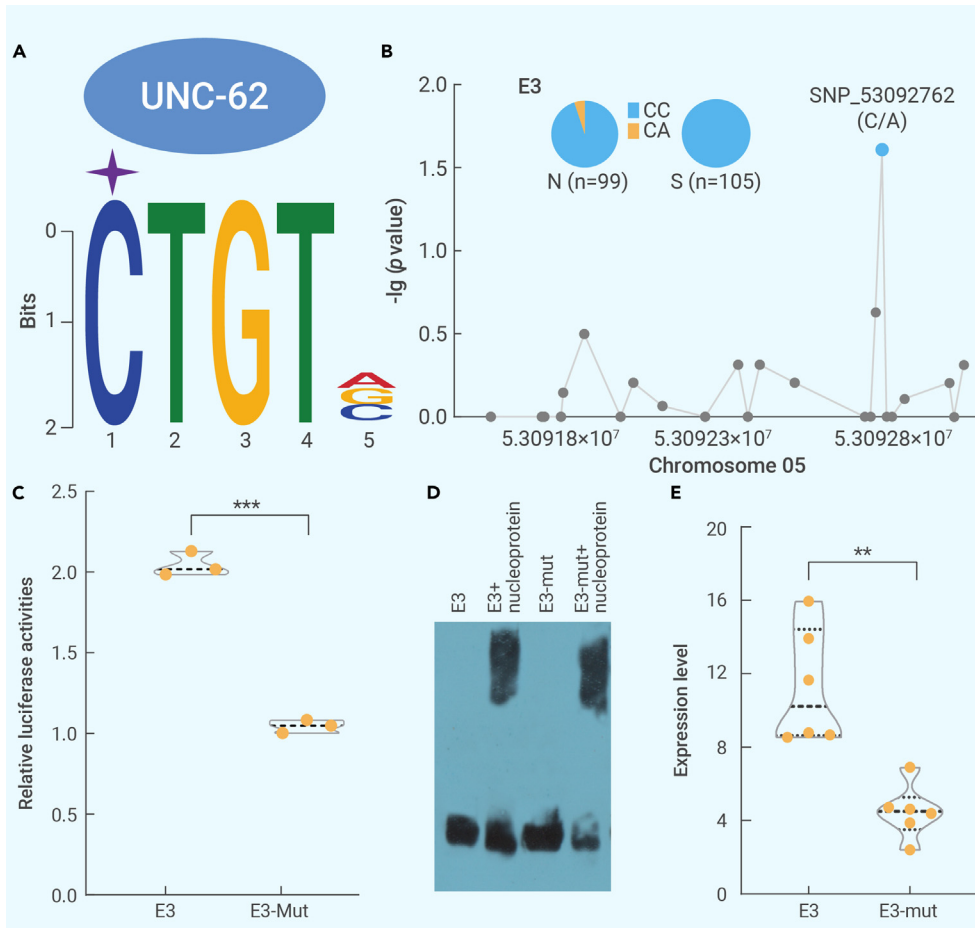


Figure 4. Genetic regulation of the distal enhancer (E3) for *Manlla* expression (A) Motif sequence and predicted binding transcription factor in E3. The star indicates that the genotype frequency of this locus was significantly different between the northern and southern oyster populations. (B) Divergence in genotype frequency of SNPs in E3 between northern and southern oyster populations. The y axis represents \log_{10} -transformed p values of the χ^2 test. Embedded pie graphs indicate allele frequencies of this SNP in the northern (N) and southern (S) native oysters. (C) Transcriptional activity of wild-type and mutant E3 using a Dual-Luciferase Reporter Assay System in human 293T cells (n = 3). (D) Binding capacity of wild-type and mutant E3 with nucleoproteins using an electrophoretic mobility shift assay. (E) Expression level of *Manlla* in oysters with or without mutated E3. Mut in (C–E) indicates E3 with C-to-A mutations. Asterisks indicate significant differences (** $p < 0.001$, two-sided Student's t test without multiple comparisons).

the C allele, whereas 5.1% of northern oysters had the heterozygous CA genotype ($p = 0.026$; Figure 4B). A dual-luciferase reporter assay detected a significant 0.48-fold reduction in transcriptional activity ($p < 0.001$) (Figure 4C).

To further examine whether this mutation affects the binding capacity of E3, we conducted an electrophoretic mobility shift assay and found a faster shift in the nucleoprotein with the mutated E3 than with the dominant CC E3 genotype (Figure 4D). Furthermore, oysters with the C-to-A mutation had a significantly decreased *Manlla* expression (2.51-fold) compared with CC oysters ($p = 0.0022$; Figure 4E).

Functions of *Manlla* and *lincRNA_E3* in shell closure and environmental response

Tissue-specific gene expression showed that *Manlla* had significantly higher expression in smooth muscle than in other tissues ($p < 0.05$; Figure S10). We performed RNA interference (RNAi) experiments to investigate whether *Manlla* and *lincRNA_E3* affect smooth muscle and shell closure. The expression levels of *Manlla* and *lincRNA_E3* were significantly decreased in RNAi-treated oysters compared with control oysters ($p < 0.01$; Figure 5A). The *Manlla*-RNAi oysters contained significantly higher mannose-containing glycan content than the control oysters ($p < 0.01$; Figure 5B). The anatomical structure of smooth muscle in *Manlla*-RNAi oysters became less compact than that in control oysters upon visual inspection (Figure 5C). Histological sections confirmed loose and twisted smooth muscle in the *Manlla*-RNAi oysters (Figure 5D), with significantly wider fiber intervals than those in controls ($p < 0.01$; Figure 5E). Furthermore, the *Manlla*-RNAi oysters exhibited a significantly weaker muscle adducting tension than the control oysters ($p < 0.01$; Figure 5F). We further found that the *Manlla*-RNAi oysters showed decreased survival post-acute heat stress (Figure 5G).

Inverse responses were detected in the *lincRNA_E3*-RNAi-treated oysters. In detail, they exhibited a significantly decreased mannose-containing glycan content ($p < 0.01$; Figure 5B), compact fiber intervals and smooth muscle structure (Figures 5C–5E), significantly strengthened muscle tension, and increased survival compared with the control and *Manlla*-RNAi oysters ($p < 0.05$; Figures 5F and 5G).

anatomical structures (Figure S11D) and histological sections (Figure S11E) between northern and southern oysters by visual inspection, oysters that survived in the southern environment had significantly smaller smooth muscle fiber intervals (Figure S11F) and stronger tension force than those that survived in the north ($p = 0.0013$; Figure S11G).

DISCUSSION

In this study, we revealed that the oyster genome is organized into higher-order 3D architecture, including compartments and TADs, a prevalent epigenetic feature in model species that is critical for many cellular processes and the regulation of gene expression.^{20–24} Genes located in A compartments exhibited high gene density and expression levels, suggesting that compartmentalization in the oyster genome may be governed by the same evolutionary tenet as tercolous plants²¹ and animals,^{24,46} which is supposed to be responsible for evolutionary adaptation to environmental gradients. Although gene density at TAD boundaries was higher than that in the intra-TAD regions, they showed no expression differences. We speculate that the small sample size may have influenced this result, which differed from previous studies reporting that genes at the TAD boundaries showed high expression levels in model species.^{20,23} In addition, 3D genome architecture was sensitive to environmental translocation, especially for regions of TAD boundaries. These topological changes were contemporary responses to environmental translocation, and further research is needed to assess whether these changes can be inherited by next generations as an evolutionary adaptation; an example is induced DNA methylation that showed transgenerational inheritance for two generations in oysters.^{47,48} High open chromatin peaks that could potentially interact with regulatory elements were enriched in the TAD boundaries, which may contribute to the high flexibility of TAD alterations. Genes near open or accessible regions showed high expression levels, and more than half of the DEGs were adjoined with open regions (intergenic regions). This provides further evidence that non-coding genomic regions play an important role in regulating downstream gene expression in response to environmental change.^{9,10} In addition, divergent expression pattern of DEGs with 3D structure alterations (compartments and

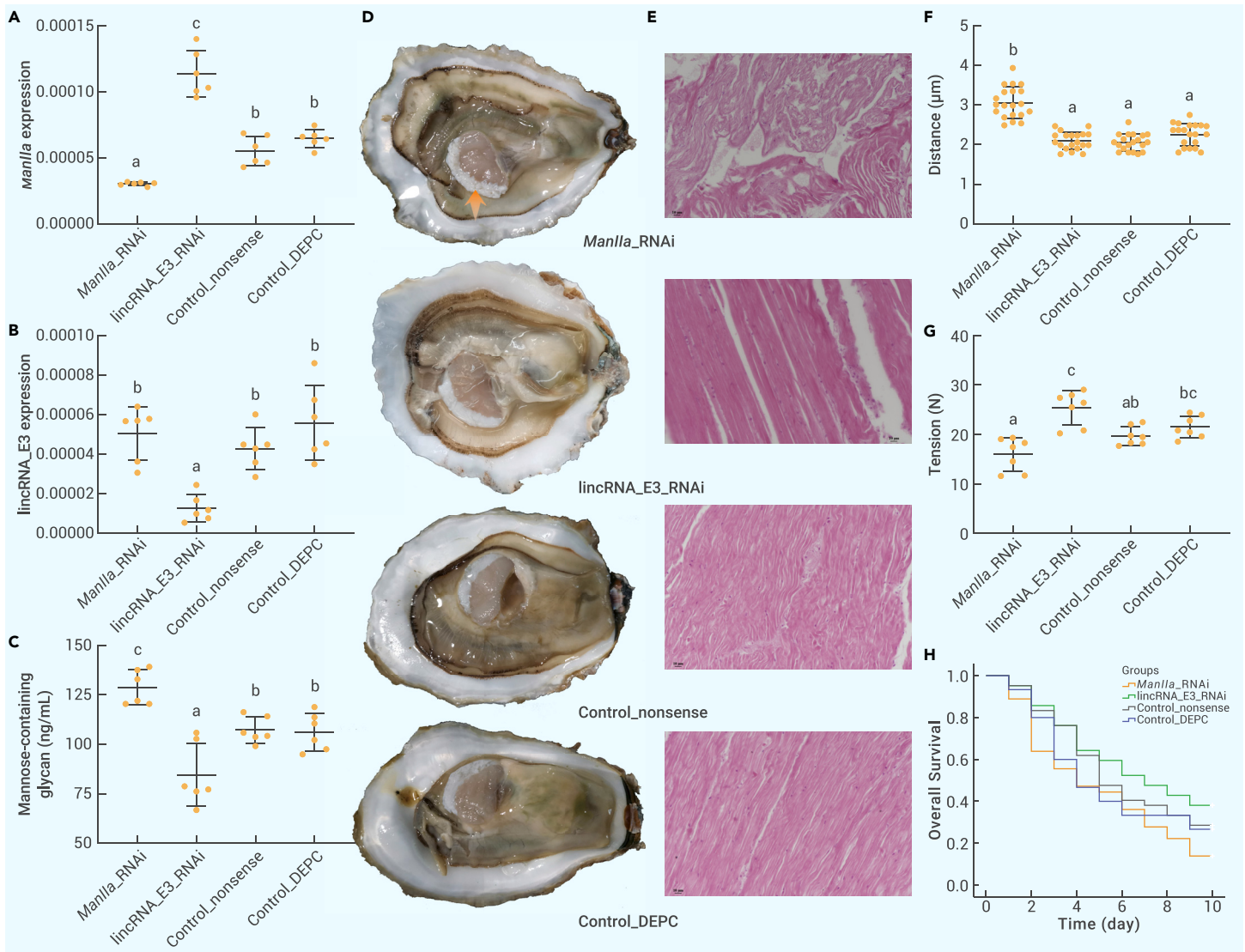


Figure 5. Functions of *Manilla* and *lincRNA_E3* in regulating mannose-containing glycan content, smooth muscle structure, and shell closure (A and B) Expression level of *Manilla* (A) and *lincRNA_E3* (B) in the smooth muscle of oysters treated with injections of *Manilla*_RNAi, *lincRNA_E3*_RNAi, nonsense dsRNA sequences, or DEPC water. (C and D) (C) Content of mannose-containing glycan in and (D) anatomical structure of oyster smooth muscle of four treatments. The orange arrow shows loose and twisted smooth muscle (photo by A.L.). (E) Histological sections of oyster smooth muscle after RNAi treatments. (F) Distance of smooth muscle fiber intervals of four treatments. (G) Muscle tension in oysters after RNAi treatments. (H) Survival post-acute heat stress (41°C for 1 h) of oysters after 10 days of recovery after RNAi treatments. Different letters indicate significant differences ($p < 0.05$, ANOVA).

TAD switch) or adjacent to accessible regions was detected where genes involved in lipolysis (fatty acid degradation), and carbohydrate metabolism (glycolysis, pyruvate metabolism and the citrate cycle) were highly expressed in non-native southern and native northern environments, respectively. Considering the large temperature difference between the two locations, our findings indicate that energy metabolism comprise a common strategy for the adaptation of marine species to temperature disturbance.^{49,50} We propose that the temperature difference contributes to alterations in the 3D genome configuration of genes responsible for energy metabolism, whereas different energetic pathways play important roles in the adaptive responses of oysters to high- and low-temperature conditions.^{10,51}

We found that the dynamics of 3D genome architecture underlie the transcriptional plasticity of estuarine oysters when translocated to new environments. The 3D response regions that were organized into A compartments and TAD boundaries after translocation enhanced gene expression plasticity. However, genes under directional selection showed limited plasticity. These findings suggest that chromosomes under strong directional selection have a limited capacity to respond positively to tremendous environmental changes that have not been experienced in the recent past. The intensity of selection and environmental difference determines the nature of the plasticity of organisms when responding to changing conditions.^{3,7,8,14} We speculate that strong

genetic differentiation and dramatic environmental changes could result in maladaptive plastic responses when oysters from northern habitats are subjected to a non-native southern environment.^{9,36} Thus, plastic changes cannot bring oysters closer to optimal fitness, resulting in a mismatch between the induced phenotype (gene expression) and the environment. Although directional selection acts on the selective sweep regions of northern oysters and favors genes that are sensitive to environmental cues, it was specifically responsible for adaptation to northern habitats.⁹ Thus, there were insufficient standing or cryptic genomic variations around selective signals in northern oysters for plastic responses to such short-term transplantation to non-native conditions. This robust negative correlation indicates a trade-off between 3D response regions and selective signals in shaping gene expression plasticity, which may be a general mechanism critical for environmental responses.^{7,13}

Our data showed that some chromosomes are specialized to respond rapidly to environmental change. In chromosomes 5 and 10, the genes in 3D response regions and regions gaining access showed greater transcriptional plasticity than those of the other chromosomes in response to short-term environmental translocation. However, they exhibited lower selective sweep signals during long-term adaptive evolution. Thus, genes in some designated chromosomes are responsible for most plastic responses that are dominated by 3D genome topology. This finding provides insight into the regulatory mechanism

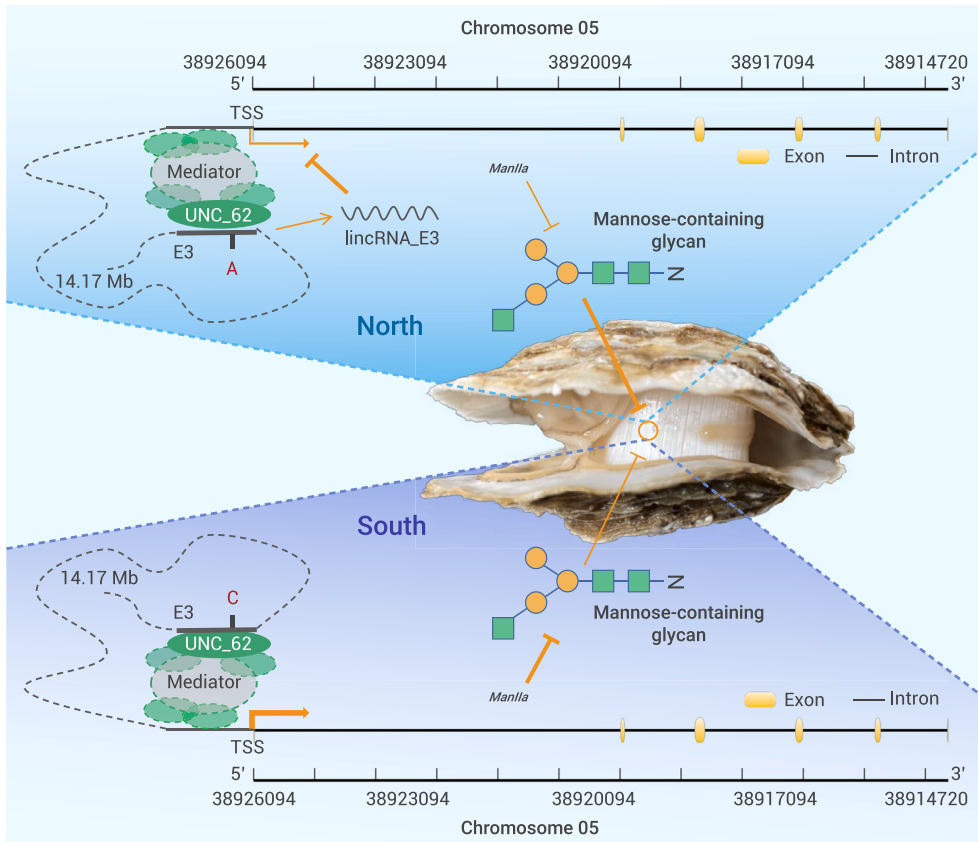


Figure 6. Schematic diagram of shell closure regulation in oyster Shell closure is controlled by smooth muscle, mannose-containing glycan, *ManIIa*, and distal enhancer (E3), as well as the environmental conditions. A point mutation (C to A) in E3 relaxes its binding capacity to transcription factors (such as UNC_62), resulting in a decrease in *ManIIa* expression. The lincRNA transcribed from E3 could also repress the expression of *ManIIa* in the north site. Upregulation of *ManIIa* expression decreased the levels of mannose-containing glycans, enforced smooth muscle structure, and subsequently strengthened shell closure (photo by C.W.).

weakens the shell closure of oysters and decreases survival under environmental stress. These results indicate that *ManIIa* is critical for and is conserved in motor function, whereas silencing *ManIIa* can result in disturbances in muscular atrophy⁵⁵ and survival.^{57–59} Moreover, the upregulation of *ManIIa* transcription may play other roles in the environmental responses of oysters by enhancing protein folding and stability, as heat shock proteins are upregulated by environmental stress.^{30,31}

This study provides an overview of the genomic landscape, including 3D configurations and selective signals, of a model marine species subjected to environmental change. Our results demonstrated that active regions in 3D genome configurations enhance transcriptional plasticity, whereas those under selection limit transcriptional plasticity.

of maladaptive plasticity and its relationship with natural selection in a model marine species.^{9,13}

We provided an interesting case showing that the interaction between 3D genome architecture and selective locus regulates the expression plasticity of a key gene responsible for a fitness-related trait. The interaction between the distal enhancer and *ManIIa* was formed/reinforced, and the chromatin was more accessible after translocation to a non-native environment, which may have potentially upregulated *ManIIa* expression and strengthened shell closure for survival. However, a point mutation (C to A) in the transcription factor-binding motif of this enhancer was identified. We speculate that this mutation affects chromatin topology and accessibility, thus relaxing its capacity to bind with transcription factors and cofactors and decreasing the transcriptional activity of this enhancer, thus resulting in downregulated *ManIIa* expression. For oysters used in multi-omic analysis, although they showed the same genotype of C/C in both the north and south environments, the newly formed or enhanced interaction, increased accessibility, and gene expression could be induced by drastic environmental changes. Furthermore, this point mutation was specifically found in oysters derived from native northern habitats. The lincRNA transcribed from this enhancer, which negatively regulates *ManIIa* expression, was also specifically highly expressed in the native northern environment. We speculate that shell closure may not be critical in the moderate or colder northern environment; thus, selection can endure oysters with a heterozygous enhancer that may be with a lower evolutionary cost than that in a homozygote³² and help those with a relatively lower *ManIIa* expression can also survive. Besides, critical role of lincRNA suggests that trait-associated lincRNAs were generally derived from enhancer regions and play an important role in transcriptional regulation.⁵² Future work will be necessary to directly clarify how variations in enhancers (such as point mutations in and lincRNA transcribed from the E3) affect 3D genome architecture and downstream gene expression.

ManIIa is a key enzyme that catalyzes mannose removal in the N-linked glycosylation of proteins.^{53,54} Silencing *ManIIa* can lead to the accumulation of mannose-containing glycans in oysters.⁵⁵ The loose and twisted smooth muscle structure observed in *ManIIa* RNAi oysters indicates that high levels of mannose-containing glycan may repress muscle growth by competitively binding to mannose receptors with high affinity, which inhibits myoblast-myotube fusion by decreasing myoblast motility.⁵⁶ Dysfunction of smooth muscle

We suggest that a trade-off or complementarity between 3D genome topology and selective signals may be a central evolutionary tenet for environmental adaptation. We found that the interaction between 3D genome architecture and selective loci regulates the gene expression plasticity of a focal fitness-related trait. The 3D configuration changes after translocation to a new environment yielded/enhanced the interaction between *ManIIa* and its enhancer, which leads to upregulated *ManIIa* transcription but further negatively regulated by a mutation and lincRNA from the enhancer. In addition, we revealed the conserved function of *ManIIa* in muscle growth. Upregulated *ManIIa* expression decreased the levels of mannose-containing glycans, promoted smooth muscle structure, and subsequently strengthened shell closure (Figure 6), which is critical to the survival of the estuarine oyster. Our findings highlights the importance of the 3D genome architecture in facilitating transcriptional plastic responses to a new environment and its compensatory interaction with selective signals in shaping plasticity under directional selection, thereby advancing our understanding of the relationship between plasticity and natural selection. Our results further provide insights into the complex genetic and epigenetic interactions critical for fitness-related traits and environmental adaptation of marine species.

MATERIALS AND METHODS

See supplemental information for details.

REFERENCES

- Whitman, D.W., and Agrawal, A.A. (2009). What Is Phenotypic Plasticity and Why Is it Important? (Science Publishers).
- Pfennig, D.W., Wund, M.A., Snell-Rood, E.C., et al. (2010). Phenotypic plasticity's impacts on diversification and speciation. *Trends Ecol. Evol.* **25**, 459–467.
- Fischer, E.K., Ghalambor, C.K., and Hoke, K.L. (2016). Can a network approach resolve how adaptive vs nonadaptive plasticity impacts evolutionary trajectories? *Integr. Comp. Biol.* **56**, 877–888.
- Oostra, V., Saastamoinen, M., Zwaan, B.J., et al. (2018). Strong phenotypic plasticity limits potential for evolutionary responses to climate change. *Nat. Commun.* **9**, 1005.
- Ghalambor, C.K., Hoke, K.L., Ruell, E.W., et al. (2015). Non-adaptive plasticity potentiates rapid adaptive evolution of gene expression in nature. *Nature* **525**, 372–375.
- Levis, N.A., and Pfennig, D.W. (2016). Evaluating 'plasticity-first' evolution in nature: Key criteria and empirical approaches. *Trends Ecol. Evol.* **31**, 563–574.
- Kelly, M. (2019). Adaptation to climate change through genetic accommodation and assimilation of plastic phenotypes. *Philos. Trans. R. Soc. Lond. B Biol. Sci.* **374**, 20180176.

8. Diamond, S.E., and Martin, R.A. (2016). The interplay between plasticity and evolution in response to human-induced environmental change. *F1000Res.* **5**, 2835.
9. Li, A., Dai, H., Guo, X., et al. (2021). Genome of the estuarine oyster provides insights into climate impact and adaptive plasticity. *Commun. Biol.* **4**, 1287.
10. Li, A., Li, L., Zhang, Z., et al. (2021). Noncoding variation and transcriptional plasticity promote thermal adaptation in oysters by altering energy metabolism. *Mol. Biol. Evol.* **38**, 5144–5155.
11. Li, L., Li, A., Song, K., et al. (2018). Divergence and plasticity shape adaptive potential of the Pacific oyster. *Nat. Ecol. Evol.* **2**, 1751–1760.
12. Schneider, R.F., and Meyer, A. (2017). How plasticity, genetic assimilation and cryptic genetic variation may contribute to adaptive radiations. *Mol. Ecol.* **26**, 330–350.
13. Becker, D., Barnard-Kubow, K., Porter, R., et al. (2022). Adaptive phenotypic plasticity is under stabilizing selection in *Daphnia*. *Nat. Ecol. Evol.* **6**, 1449–1457.
14. Ho, W.C., and Zhang, J. (2018). Evolutionary adaptations to new environments generally reverse plastic phenotypic changes. *Nat. Commun.* **9**, 350.
15. West-Eberhard, M.J. (2003). *Developmental Plasticity and Evolution* (Oxford University Press).
16. West-Eberhard, M.J. (2005). Developmental plasticity and the origin of species differences. *Proc. Natl. Acad. Sci. USA* **102**, 6543–6549.
17. Rickels, R., and Shilatfard, A. (2018). Enhancer logic and mechanics in development and disease. *Trends Cell Biol.* **28**, 608–630.
18. Grishkevich, V., and Yanai, I. (2013). The genomic determinants of genotype \times environment interactions in gene expression. *Trends Genet.* **29**, 479–487.
19. Jerkovic, I., and Cavalli, G. (2021). Understanding 3D genome organization by multidisciplinary methods. *Nat. Rev. Mol. Cell Biol.* **22**, 511–528.
20. Liu, C., Cheng, Y.J., Wang, J.W., et al. (2017). Prominent topologically associated domains differentiate global chromatin packing in rice from Arabidopsis. *Nat. Plants* **3**, 742–748.
21. Wang, M., Wang, P., Lin, M., et al. (2018). Evolutionary dynamics of 3D genome architecture following polyploidization in cotton. *Nat. Plants* **4**, 90–97.
22. Zheng, H., and Xie, W. (2019). The role of 3D genome organization in development and cell differentiation. *Nat. Rev. Mol. Cell Biol.* **20**, 535–550.
23. Dixon, J.R., Selvaraj, S., Yue, F., et al. (2012). Topological domains in mammalian genomes identified by analysis of chromatin interactions. *Nature* **485**, 376–380.
24. Fishman, V., Battulin, N., Nuriddinov, M., et al. (2019). 3D organization of chicken genome demonstrates evolutionary conservation of topologically associated domains and highlights unique architecture of erythrocytes' chromatin. *Nucleic Acids Res.* **47**, 648–665.
25. Corces, M.R., Trevino, A.E., Hamilton, E.G., et al. (2017). An improved ATAC-seq protocol reduces background and enables interrogation of frozen tissues. *Nat. Methods* **14**, 959–962.
26. Davies, J.O.J., Oudelaar, A.M., Higgs, D.R., et al. (2017). How best to identify chromosomal interactions: A comparison of approaches. *Nat. Methods* **14**, 125–134.
27. Bonev, B., and Cavalli, G. (2016). Organization and function of the 3D genome. *Nat. Rev. Genet.* **17**, 661–678.
28. Leimar, O., Dall, S.R.X., McNamara, J.M., et al. (2019). Ecological genetic conflict: Genetic architecture can shift the balance between local adaptation and plasticity. *Am. Nat.* **193**, 70–80.
29. Walter, G.M., Clark, J., Terranova, D., et al. (2023). Hidden genetic variation in plasticity provides the potential for rapid adaptation to novel environments. *New Phytol.* **239**, 374–387.
30. Guo, X., He, Y., Zhang, L., et al. (2015). Immune and stress responses in oysters with insights on adaptation. *Fish Shellfish Immunol.* **46**, 107–119.
31. Zhang, G., Fang, X., Guo, X., et al. (2012). The oyster genome reveals stress adaptation and complexity of shell formation. *Nature* **490**, 49–54.
32. Guo, X., Li, C., Wang, H., et al. (2018). Diversity and evolution of living oysters. *J. Shellfish Res.* **37**, 755–771.
33. Sanford, E., and Kelly, M.W. (2011). Local adaptation in marine invertebrates. *Ann. Rev. Mar. Sci.* **3**, 509–535.
34. Somero, G.N. (2012). The physiology of global change: Linking patterns to mechanisms. *Ann. Rev. Mar. Sci.* **4**, 39–61.
35. Bozinovic, F., Calosi, P., and Spicer, J.I. (2011). Physiological correlates of geographic range in animals. *Annu. Rev. Ecol. Syst.* **42**, 155–179.
36. Li, A., Wang, C., Wang, W., et al. (2020). Molecular and fitness data reveal local adaptation of southern and northern estuarine oysters (*Crassostrea ariakensis*). *Front. Mar. Sci.* **7**.
37. Nagai, K., Honjo, T., Go, J., et al. (2006). Detecting the shellfish killer *Heterocapsa circularis-quama* (Dinophyceae) by measuring bivalve valve activity with a Hall element sensor. *Aquaculture* **255**, 395–401.
38. Poulet, S.A., Lennon, J.-F., Plouvenez, F., et al. (2003). A nondestructive tool for the measurement of muscle strength in juvenile oysters *Crassostrea gigas*. *Aquaculture* **217**, 49–60.
39. Lombardi, S.A., Harlan, N.P., and Paynter, K.T. (2013). Survival, Acid–Base Balance, and Gaping Responses of the Asian Oyster *Crassostrea ariakensis* and the Eastern Oyster *Crassostrea virginica* During Clamped Emersion and Hypoxic Immersion. *J. Shellfish Res.* **32**, 409–415.
40. Fisher, R.A. (2006). Initial Market Assessment of the Cultured, Non-native Oyster *C. Ariakensis* (Virginia Institute of Marine Science). Marine Resource Report.
41. Guévelou, E., Huvet, A., Sussarellu, R., et al. (2013). Regulation of a truncated isoform of AMP-activated protein kinase α (AMPK α) in response to hypoxia in the muscle of Pacific oyster *Crassostrea gigas*. *J. Comp. Physiol. B* **183**, 597–611.
42. Chantler, P.D. (2006). Scallop adductor muscles: Structure and function. *Dev. Aquac. Fish. Sci.* **35**, 229–316.
43. Takahashi, I., Shimada, M., Akimoto, T., et al. (2003). Electron microscopic evidence for the thick filament interconnections associated with the catch state in the anterior byssal retractor muscle of *Mytilus edulis*. *Comp. Biochem. Physiol. Mol. Integr. Physiol.* **134**, 115–120.
44. Rao, S.S.P., Huntley, M.H., Durand, N.C., et al. (2014). A 3D map of the human genome at kilobase resolution reveals principles of chromatin looping. *Cell* **159**, 1665–1680.
45. Lieberman-Aiden, E., van Berkum, N.L., Williams, L., et al. (2009). Comprehensive mapping of long-range interactions reveals folding principles of the human genome. *Science* **326**, 289–293.
46. Kaaij, L.J.T., van der Weide, R.H., Ketting, R.F., et al. (2018). Systemic loss and gain of chromatin architecture throughout zebrafish development. *Cell Rep.* **24**, 1–10.e4.
47. Wang, X., Li, A., Wang, W., et al. (2021). Direct and heritable effects of natural tidal environments on DNA methylation in Pacific oysters (*Crassostrea gigas*). *Environ. Res.* **197**, 111058.
48. Wang, X., Cong, R., Li, A., et al. (2023). Transgenerational effects of intertidal environment on physiological phenotypes and DNA methylation in Pacific oysters. *Sci. Total Environ.* **871**, 162112.
49. Tomanek, L. (2014). Proteomics to study adaptations in marine organisms to environmental stress. *J. Proteomics* **105**, 92–106.
50. Sokolova, I.M., Frederich, M., Bagwe, R., et al. (2012). Energy homeostasis as an integrative tool for assessing limits of environmental stress tolerance in aquatic invertebrates. *Mar. Environ. Res.* **79**, 1–15.
51. Li, A., Li, L., Song, K., et al. (2017). Temperature, energy metabolism, and adaptive divergence in two oyster subspecies. *Ecol. Evol.* **7**, 6151–6162.
52. Ransohoff, J.D., Wei, Y., and Khavari, P.A. (2018). The functions and unique features of long intergenic non-coding RNA. *Nat. Rev. Mol. Cell Biol.* **19**, 143–157.
53. Shah, N., Kuntz, D.A., and Rose, D.R. (2008). Golgi alpha-mannosidase II cleaves two sugars sequentially in the same catalytic site. *Proc. Natl. Acad. Sci. USA* **105**, 9570–9575.
54. Chui, D., Oh-Eda, M., Liao, Y.F., et al. (1997). Alpha-mannosidase-II deficiency results in dyserythropoiesis and unveils an alternate pathway in oligosaccharide biosynthesis. *Cell* **90**, 157–167.
55. Malm, D., and Nilssen, Ø. (2008). Alpha-mannosidosis. *Orphanet J. Rare Dis.* **3**, 21.
56. Jansen, K.M., and Pavlath, G.K. (2006). Mannose receptor regulates myoblast motility and muscle growth. *J. Cell Biol.* **174**, 403–413.
57. Rose, D.R. (2012). Structure, mechanism and inhibition of Golgi alpha-mannosidase II. *Curr. Opin. Struct. Biol.* **22**, 558–562.
58. Paschinger, K., Hackl, M., Gutternigg, M., et al. (2006). A deletion in the Golgi alpha-mannosidase II gene of *Caenorhabditis elegans* results in unexpected non-wild-type N-glycan structures. *J. Biol. Chem.* **281**, 28265–28277.
59. Walski, T., Van Damme, E.J.M., Smargiasso, N., et al. (2016). Protein N-glycosylation and N-glycan trimming are required for postembryonic development of the pest beetle *Tribolium castaneum*. *Sci. Rep.* **6**, 35151.

ACKNOWLEDGMENTS

The authors thank X.G. Wang and Y. Peng for oyster sampling, H. Song, X.T. Wang, and W. Wang (Ludong University) for RNAi and shell tension experiments, and Q. Liu, H. Zhao, and L. Wu for the histology experiment. This work was supported by the National Key Research and Development Program of China (2022YFD2400304 to L.L.), the National Natural Science Foundation of China (32101353 to A.L.), the Youth Innovation Promotion Association, Chinese Academy of Sciences (2023215 to A.L.), the Strategic Priority Research Program of the Chinese Academy of Sciences (XDA23050402 to L.L.), the Young Elite Scientists Sponsorship Program by the China Association for Science and Technology (2021QNRC001 to A.L.), the Key Research and Development Program of Shandong (2022LZGC015 to L.L.), the China Agriculture Research System of MOF and MARA (CARS-49 to L.L.), and the USDA NIFA Hatch Animal Health Project (NJ32920 to X.G.).

AUTHOR CONTRIBUTIONS

L.L. and G.Z. conceived the study. A.L. carried out the data analysis and drafted the manuscript. A.L. contributed to the Hi-C and ATAC-seq analyses. A.L., M.Z., C.W., and X.W. contributed to the gene function experiments. A.L., M.Z., X.Z., and J.G. contributed to the Tn5-FISH analysis. A.L., W.W., Z.Z., and K.Z. contributed to the collection, translocation, and sampling of the oysters. L.L., X.G., and G.Z. participated in the final data analysis, interpretation, and manuscript writing. A.L., X.G., P.R.d.W., L.L., and G.Z. revised the manuscript. All authors have read and approved the manuscript for publication.

DECLARATION OF INTERESTS

The authors declare no competing interests.

DATA AVAILABILITY

All raw sequencing data generated in this study, including those from the Hi-C, ATAC-seq, and RNA-seq, have been deposited with the BioProject database (<http://www.ncbi.nlm.nih.gov/bioproject>) under the accession no. PRJNA832508.

SUPPLEMENTAL INFORMATION

Supplemental information can be found online at <https://doi.org/10.1016/j.xinn.2023.100464>.

LEAD CONTACT WEBSITE

http://english.qdio.cas.cn/people/jzg/202208/t20220804_310248.html